Short- and Long-Range Interactions in Thin Films of Polymer Blends in Microchannels

Pil Jin Yoo, K. Y. Suh, and Hong H. Lee*

School of Chemical Engineering, Seoul National University, Seoul 151-742, Korea

Received September 10, 2001

ABSTRACT: We present the surface structures formed under the void microchannels of an elastomeric mold when thin films of polystyrene/polybutadiene (PS/PB) blends are annealed with the mold placed on the film. Exactly opposite types of structure result under identical annealing conditions, depending only on the height difference in the as-cast thin film between the PS and PB phases. Recessed patterns form under the microchannel by long-range interactions when this height is more than 60 nm; the usual protruding patterns result in the void microchannels due to the short-range interactions of capillarity when the height is less than 40 nm. The height of fully developed meniscus of the mobile PB in solid PS is believed to be the factor that determines the type of pattern formation.

I. Introduction

Thin films of polymer blends have received much attention because of their technological importance in dielectrics, photoresists, optics, lubrication, adhesives, and others. One of earlier studies looked into the effect of surface on spinodal decomposition.[1] Tanaka dealt with the interplay between wetting and phase separation of a binary mixture confined by walls.[2] Phase separation of spin-cast films of polymer blends was studied by a number of investigators[3−5] for their surface structure and morphology. The effect of mechanical confinement on the phase separation was also explored.[6] The confinement effect on the phase separation[7] was investigated with a system in which molded strips of polymer blends provide the lateral confinement.

The wetting and phase separation have to do with short-range interactions of capillarity as opposed to long-range interactions, which involve van der Waals forces. These long-range interactions have been extensively explored in spinodal dewetting of thin polymer films.[8−10] While there have been numerous studies in which short- or long-range interactions alone play the major role in thin polymer films, there has been little study in which both interactions interplay. One major reason has to do with the difficulty of finding such a system.

Recently, we developed a new lithographic technique called "capillary force lithography" (CFL).[11] In this technique, a patterned elastomeric mold such as poly(dimethylsiloxane) (PDMS) mold is placed on a polymer film spin-coated onto a substrate, and the temperature is raised above the glass transition temperature of the polymer. During the annealing, capillary force allows the polymer melt to fill up the void space of the channels formed between the mold and the polymer film, thereby generating the negative replica of the mold.

Application of CFL to thin films of polymer blends could provide one with a system in which there is an interplay between short- and long-range interactions. In this paper, we investigate such a system involving blends of polystyrene (PS) and polybutadiene (PB). This conventional immiscible blend system is chosen because of a large difference in the glass transition temperature (T_g = 100 °C for PS and −95 °C for PB) and a relatively small difference in the surface tension (40 mN/m for PS and 32 mN/m for PB).

There can be two operating windows of annealing for the binary blend, i.e., $T_{g,b} < T < T_{g,s}$ and $T > T_{g,s}$, where $T_{g,b}$ is the glass transition temperature of PB and $T_{g,s}$ is that of PS. In the case of $T > T_{g,s}$, the interplay between short- and long-range interactions cannot be observed since then both PS and PB are mobile. Therefore, the operating window of $T_{g,b} < T < T_{g,s}$ is chosen for this study. In this way, the component of lower T_g would feel both the lateral barrier effect from the other immobile component and the axial confinement effect from the patterned mold.

II. Experimental Section

Film Preparation. Polymers used in this study are PS (M_W = 280K, T_g = 100 °C) and PB (M_W = 420K, T_g = −95 °C) purchased from Aldrich. Polymer films were obtained by spin-coating PS/PB (50/50) and PS/PB (65/35) solutions onto (100) silicon substrates. The substrate was cleaned by ultrasonic treatment in trichloroethylene and methanol for 5 min each and dried in nitrogen. Native oxide was not removed from the surface and thus would exist on the surface. The film thickness was controlled by means of the solution concentration and the rotation speed in spin-coating to obtain thicknesses of about 60 and 120 nm.

Capillary Force Lithography and Surface Characterization. For the CFL process, we fabricated poly(dimethylsiloxane) (PDMS, Sylgard 184, Dow Corning) mold that has a planar surface with recessed patterns by casting PDMS against a complementary relief structure prepared by photolithographic method. The mold has a line-and-space pattern: five equally spaced line-and-space strips with a spacing of 3 μm and one isolated line, all with the same height of 550 nm. The images of the pattern obtained by contact-mode atomic force microscopy (AFM) are shown in Figure 1.

The annealing temperature in this study ranges from 80 to 95 °C. Unless otherwise noted, the data presented are those corresponding to the annealing temperature of 95 °C. This temperature was chosen to maximize the mobility of PB within the immobile PS phase. In view of earlier studies[12,13] on the effect of film thickness on the glass transition temperature (T_g), one might wonder whether the PS phase would remain in

* To whom correspondence should be addressed. E-mail: honghlee@plaza.snu.ac.kr.

10.1021/ma011602l CCC: $22.00
Published on Web 03/08/2002

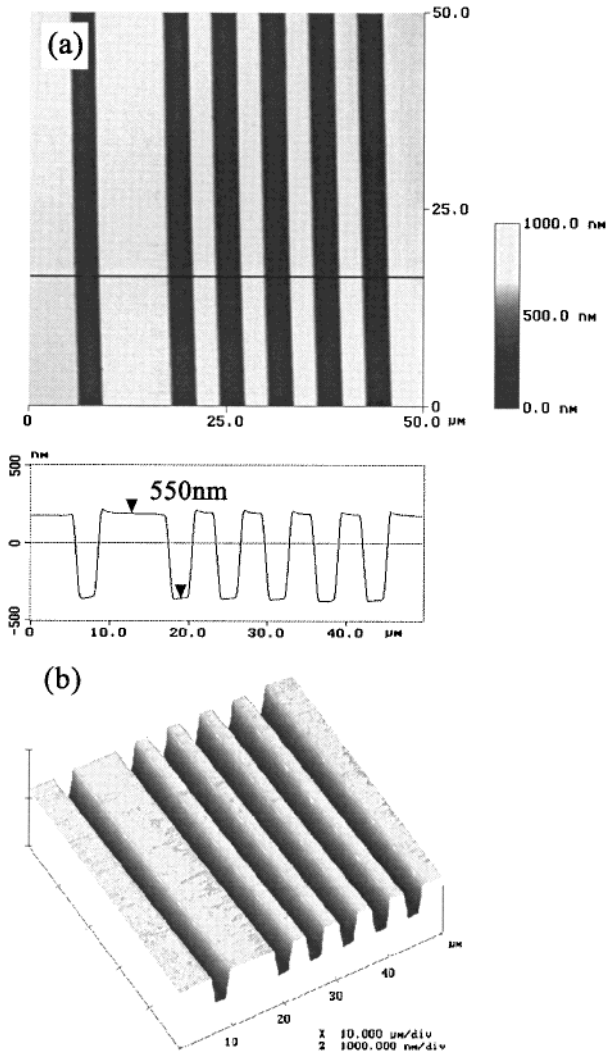

Figure 1. (a) Two-dimensional and cross-sectional atomic force microscopy (AFM) images of PDMS mold. (b) Three-dimensional AFM images of PDMS mold.

glassy state at 95 °C. For the thinnest film used in this study, the thickness is about 60 nm, which would result in a reduction of T_g by only about a few degrees. In fact, separate experiments involving only PS showed that PS is immobile at 95 °C in the sense that CFL cannot be done. Only when the thickness is reduced below 30 nm would one observe a slight movement of PS at 95 °C, as observed by CFL.

To prevent the undesirable distortion that a difference in the thermal expansion coefficient could cause between the mold and the substrate (4 μm/(cm °C) for silicon and 330 μm/(cm °C) for PDMS), the mold was placed on the substrate coated with the blend film after a thermal equilibrium is reached at 95 °C, and then the blend film was annealed for 24 h with the mold in place. After the annealing, the mold was removed at 95 °C, and the sample was allowed to cool to room temperature. The surface morphology of the sample thus obtained was examined with AFM (NanoScope IIIa, Digital Instruments) in a tapping mode to prevent any possible damage to the PB phase. Root-mean-square amplitudes of 0.6−0.8 V were used to prevent the undesired vibrational image of rubbery PB phase. All AFM data were transformed by a flattening treatment when needed to the same visual conditions for comparison.

III. Results and Discussion

We find from our experimental results that there is a capillary rise, as one would expect, of the mobile PB phase into the void of the microchannels of the mold when annealed. To our surprise, however, the region under the void of the microchannels recedes instead of rising as if pressed in by an external force under the identical annealing condition, when the initial film thickness is relatively large.

To understand the contrasting behavior, we begin in what follows with a discussion of the morphology of the as-cast film to show that the mobile PB is surrounded by immobile PS "walls", the height of which depends on the initial film thickness. When annealed, the mobile PB wets and climbs up the PS walls. If this capillary rise is sufficient enough for the risen PB to make contact with the capping PDMS walls, PB is picked up by the walls through capillarity again, and it rises into the void of the PDMS mold. If the contact is not made, on the other hand, the fate of PB is determined by the magnitude of the disjoining pressure of the film under the void relative to that of the adjacent film that is in contact with PDMS. Therefore, a discussion on the disjoining pressure follows. Since the mobile PB rises into or recedes from the void of PDMS mold depending on the relative magnitude of the capillary rise with respect to the PS wall height, finally an estimation of the capillary rise is made of PB along the PS walls to compare it with the experimental value.

(a) Surface Morphology of the As-Cast Films. AFM images of the phase-separated structures are shown for the as-cast films from a symmetric PS/PB (50/50) blend solution that are 120 ± 10 nm thick in Figure 2a and 60 ± 4 nm thick in Figure 2b. Well-known sealike and islandlike structures are seen to have formed. The darker sealike domain consists of a PB-rich phase, and the brighter islandlike domain is a PS-rich phase. If thermodynamics were the only consideration, PB segments would move to the air−polymer interface to minimize the interfacial free energy since PB segments have a lower surface tension than PS segments (40 mN/m for PS and 32 mN/m for PB). However, a surface structure similar to that resulting from spinodal decomposition forms due to a very high rate of solvent evaporation taking place in the course of spin-coating.[3−5] As a result, a local rearrangement makes the PS-rich segments protrude from the film surface as seen in Figure 2a,b.

A reversed contrast results when an asymmetric PS/PB (65/35) blend solution is used as shown in Figure 2c for a 120 nm thick film and in Figure 2d for the same but 60 nm thick film. In this case, the brighter sealike domain consists of a PS-rich phase and the darker islandlike domain is a PB-rich phase, owing to the increase in the fraction of PS component. The characteristic domain size in both cases increases with increasing film thickness, as expected.[5]

An important aspect of the as-cast film structures, as related to the discussion to follow, is that PB phase is surrounded by PS walls whether the blend composition is symmetric or asymmetric. Another aspect is that the distance between the trough and the hill of the protruding PS phase, or the height of PS walls, is about 60−70 nm for the 120 nm thick film whereas it is about 30−40 nm for the 60 nm thick film for both symmetric and asymmetric blends as shown in Figure 2. We found that this distance is larger for the thicker film.

(b) Disjoining Pressures. AFM images of the surface structures resulting from annealing are shown in Figure 3 for the 120 nm thick films prepared from the

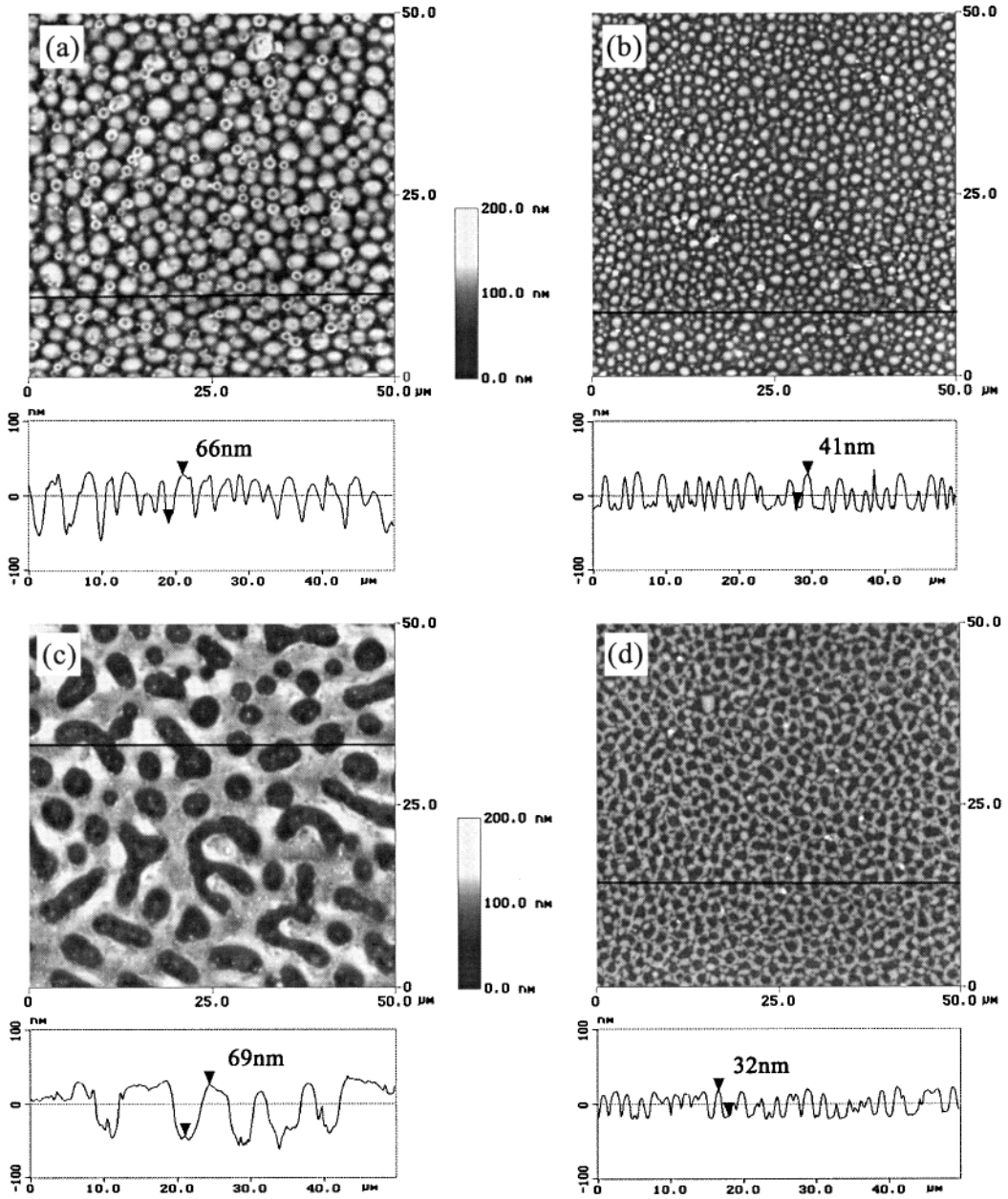

Figure 2. (a) Two-dimensional and cross-sectional AFM images of PS/PB (50/50) blend film 120 nm thick. Darker domains consist of a PB-rich phase and brighter domains are a PS-rich phase. (b) Two-dimensional and cross-sectional AFM images of PS/PB (50/50) blend film 60 nm thick. (c) Two-dimensional and cross-sectional AFM images of PS/PB (65/35) blend film 120 nm thick. (d) Two-dimensional and cross-sectional AFM images of PS/PB (65/35) blend film 60 nm thick.

symmetric (Figure 3a,c) and asymmetric (Figure 3b,d) blend solutions. The annealing was carried out with the patterned PDMS mold in place for 24 h at 95 °C. Comparison between the three-dimensional images of the mold (Figure 1b, note that the isolated line in the figure can be used as a marker for comparison) and those of the annealed films (Figure 3c,d) should reveal that the stripelike region under the void of the microchannels of the mold has receded as a result of the annealing, as if the striped region is pressed in by a mold with protruding lines. Ordinarily, one would expect a capillary rise of the mobile polymer into the void of the microchannel.

This fact suggests that the rise of the mobile PB by wetting of PS wall may not be sufficiently high enough that PB cannot make contact with the PDMS walls for the capillary rise. While this suggestion explains no capillary rise, it still does not account for the receding. Therefore, there must be a force acting on the mobile PB for it to recede.

To get an understanding of the force responsible for the receding, we examine an idealized version of the structure pictorialized in Figure 4. Two assumptions have been made in the idealization. First, two polymers have a simply shaped domain and a interface. Second, the partial presence of a very thin PS residue in the PB-rich domains is neglected as supported from Figure 2, because PB has a larger wettability to the Si/SiO_x surface than PS.[3] It is well-known in polymer dewetting that the dominant force in films thinner than 100 nm is the long-range force in the form of van der Waals interactions.[8,10,14] There are two competing forces of the same kind in Figure 4: one (ΔG_{2A}) from the silicon/PB/air (1/2/3) interactions, which corresponds to the PB

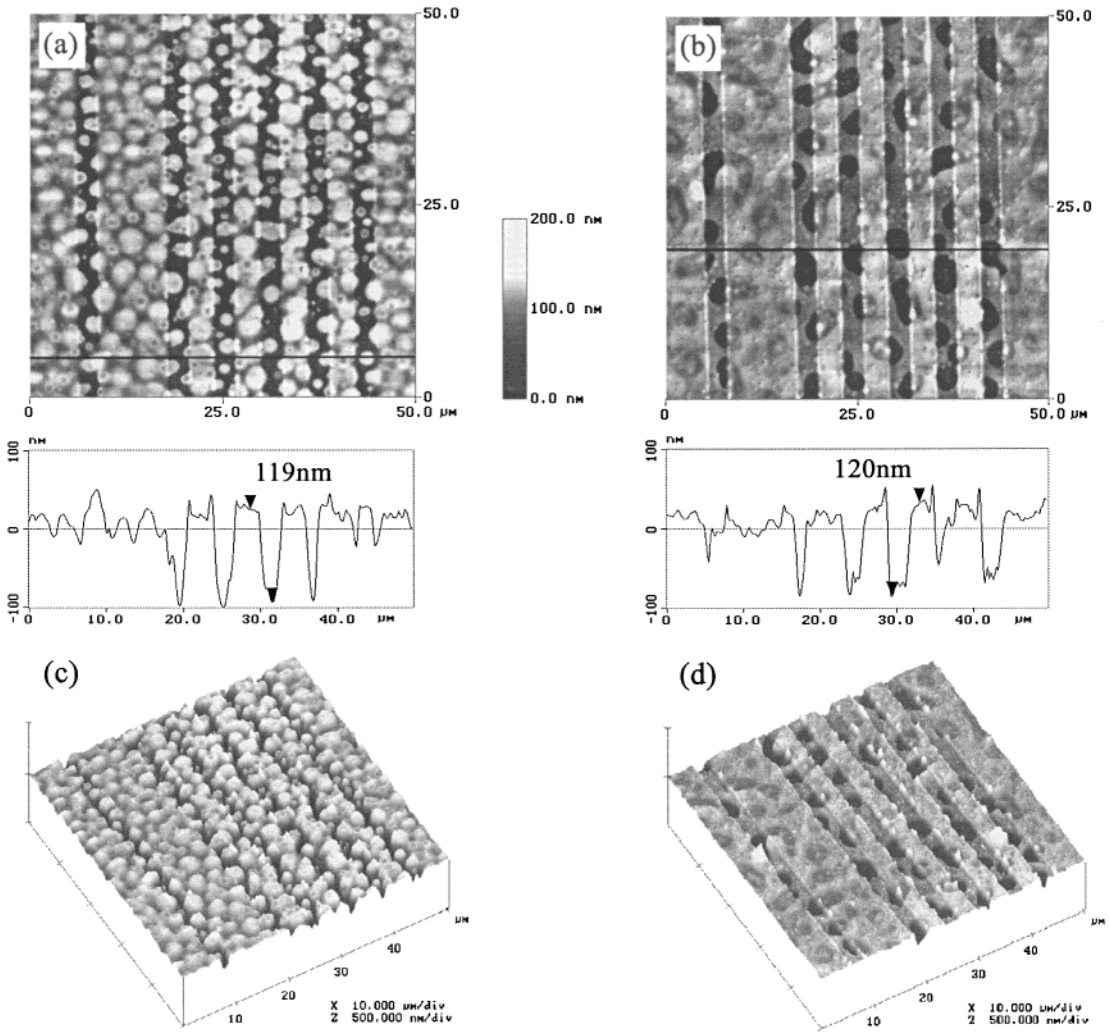

Figure 3. (a) Two-dimensional and cross-sectional AFM images of PS/PB (50/50) blend film 120 nm thick with recessed strips. (b) Two-dimensional and cross-sectional AFM images of PS/PB (65/35) blend film 120 nm thick with recessed strips. (c) Three-dimensional AFM images of PS/PB (50/50) blend film 120 nm thick with recessed strips. (d) Three-dimensional AFM images of PS/PB (65/35) blend film 120 nm thick with recessed strips.

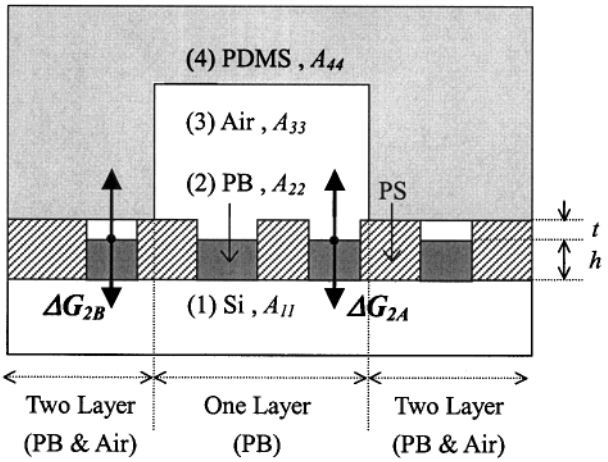

Figure 4. Idealized schematic diagram for the recessed pattern formation. Two kinds of van der Waals forces, ΔG_{2A} and ΔG_{2B}, competitively act on the PB layer.

phase in the void of the microchannel, and the other (ΔG_{2B}) from the silicon/PB/air/PDMS (1/2/3/4) interactions,[15] which corresponds to the PB phase in the region where PDMS makes contact with the underlying polymer, or contact region. The main difference between the two is that there is a very thin air layer trapped in the contact region while there is an air layer that is relatively very thick (550 nm) in the void region. Therefore, the air layer can be excluded in the energy term for the latter. Then the total excess free energies per unit area of the nonretarded van der Waals interactions between the layer 2 (PB layer) and the other layers become[15−18]

$$\Delta G_{2A} = -\frac{1}{12\pi}\frac{A_{123}}{h^2} \tag{1}$$

$$\Delta G_{2B} = -\frac{1}{12\pi}\left(\frac{A_{123}}{h^2} + \frac{A_{1234}}{(h+t)^2}\right) \tag{2}$$

where h is the thickness of PB layer, t is the thickness of a capped air layer in the contact region, and A's are the effective Hamaker constants. In eq 2, the first term represents the interactions between the silicon substrate and the air layer across the PB layer, and the second term accounts for those between the silicon substrate and the PDMS mold across the PB and air layers. The effective Hamaker constants can be expressed in terms of respective Hamaker constants for each layer to give[16]

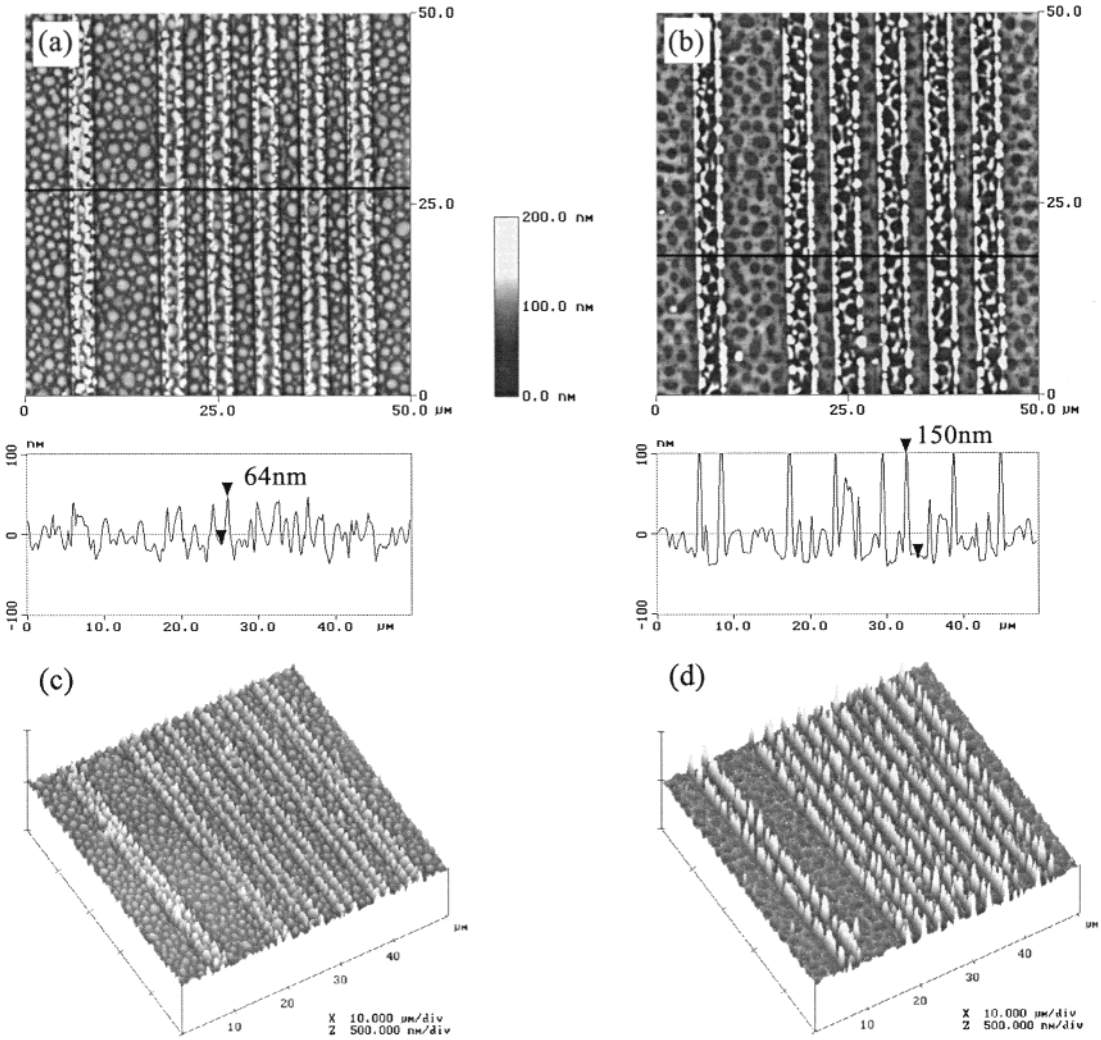

Figure 5. (a) Two-dimensional and cross-sectional AFM images of PS/PB (50/50) blend film 60 nm thick with protruding strips. (b) Two-dimensional and cross-sectional AFM images of PS/PB (65/35) blend film 60 nm thick with protruding strips. (c) Three-dimensional AFM images of PS/PB (50/50) blend film 60 nm thick with protruding strips. (d) Three-dimensional AFM images of PS/PB (65/35) blend film 60 nm thick with protruding strips.

$$A_{123} = (\sqrt{A_{11}} - \sqrt{A_{22}})(\sqrt{A_{33}} - \sqrt{A_{22}}) \quad (3)$$

$$A_{1234} = (\sqrt{A_{11}} - \sqrt{A_{22}})(\sqrt{A_{44}} - \sqrt{A_{33}}) \quad (4)$$

where the subscripts are for the layers in Figure 4. The force per unit area or the disjoining pressure is then given by[19]

$$F_{2A} = -\frac{\partial \Delta G_{2A}}{\partial h} = -\frac{1}{6\pi}\frac{A_{123}}{h^3} \quad (5)$$

$$F_{2B} = -\frac{\partial \Delta G_{2B}}{\partial h} = -\frac{1}{6\pi}\left(\frac{A_{123}}{h^3} + \frac{A_{1234}}{(h+t)^3}\right) \quad (6)$$

The sign of the Hamaker constants is of interest here. Although exact values are not available, $A_{11} < A_{22}$ such that $(\sqrt{A_{11}} - \sqrt{A_{22}})$ is negative since otherwise well-known dewetting of thin PB film on silicon substrate would not take place.[20] Although the substrate is silicon, in reality there is always a thin native oxide layer present on the silicon substrate so that the surface is essentially silicon oxide for the polymer layer on silicon. The values of Hamaker constants for silica (A_{11}) and polymer (A_{22}) are $(5.0-6.0) \times 10^{-20}$ J and $(6.5-8.0) \times 10^{-20}$ J, respectively.[21] Since the Hamaker constant of air is nearly zero, it follows from eqs 3 and 4 that A_{123} is positive whereas A_{1234} is negative. Therefore, it follows from eqs 5 and 6 that the force pushing mobile PB downward in the void region, F_{2A}, is greater than that in the contact region, F_{2B}. As a result, the PB in the void region is pushed into the PB layer in the adjacent contact regions. This tendency becomes stronger as the thickness of PB layer or h (eq 5) in the void region decreases due to the mass transport. In fact, the experimental results show that there is little PB layer left in the recessed strips as the depth of the strips is about 120 nm (Figure 3a,b) for the 120 nm thick film.

Under the identical annealing conditions, however, an exactly opposite behavior is observed for 60 nm thick film as revealed by the AFM images in Figure 5. Instead of receding, PS rises into the void of the microchannel such that protruding strips result. As discussed earlier, the only difference here is the film thickness: the trough to hill distance of the solid PS phase is about 30−40 nm for the 60 nm thick film whereas it is 60−70 nm for the 120 nm thick film (see cross-sectional profiles in Figure 2). The key, therefore, lies in whether the wetting (spreading) of PB on PS walls would allow an ascent of PB to a height that is high enough to make contact with

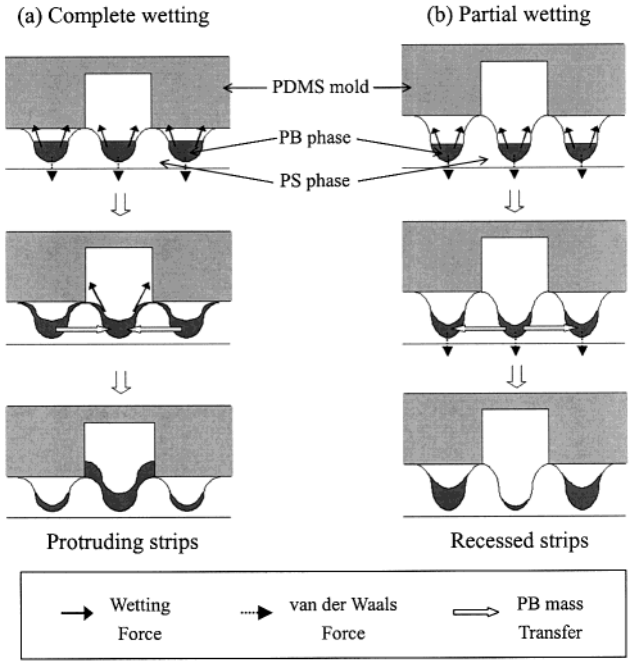

Figure 6. Idealized schematic diagram for the two types of pattern formation. Short-range interactions dominate under complete wetting condition and lead to the protruding pattern. In contrast, long-range interactions dominate under partial wetting condition and lead to the recessed pattern.

the PDMS mold. Our experimental results indicate that a trough to hill distance or a PS wall height of 30−40 nm can be covered by wetting but not a distance of 60−70 nm.

The picture emerging here is that, in the initial stage of the pattern formation, the short-range force of wetting dominates over the long-range force of van der Waals interactions such that an equilibrium capillary rise determines whether the risen PB by wetting can make contact with the PDMS walls. An idealized version of this picture is depicted in Figure 6. The case of making the contact is referred to as "complete wetting" in the figure and that of not making the contact as "partial wetting". When the equilibrium rise is sufficient to result in complete wetting, the PDMS mold picks up the risen PB and also draws PB from the adjacent contact regions for the capillary rise into the mold void, leading to the protruding pattern in Figure 6. Although there can also be a capillary rise in the microchannel in the contact regions, it is suppressed by the increased air pressure in the contact region when PB attempts to rise by capillarity, owing to too small a volume of capped air compared with that in the void of the channel of the PDMS mold. When the partial wetting occurs, the short-range force of capillarity has run its course in that the PB phase is all interconnected such that the capillary force in the void region is counterbalanced by that in the contact region. Therefore, only the long-range force of van der Waals interactions comes into play, which causes the PB in the void region to move into the contact region, resulting in the recessed pattern depicted in Figure 6 and detailed in Figure 4. Under the annealing conditions here, the equilibrium rise by wetting must be greater than 40 nm but less than 60 nm.

(c) Estimation of Capillary Rise. To get an estimate of this equilibrium rise by wetting, which should be around 50 nm, we begin with a discussion of the capillary rise of PB in an idealized rectangular PS channel. A geometrical consideration of fully developed meniscus of PB gives for the height of the meniscus, h_c, as measured from the meniscus center

$$h_c = L\left|\frac{1-\sin\theta}{\cos\theta}\right| \tag{7}$$

where L is the half channel width and θ is the contact angle, which was determined by a contact angle meter to be 21°.

There are two factors that need to be taken into consideration when applying eq 7 to the blend system for an estimate of the equilibrium rise. Unlike rectangular channels to which eq 7 is applicable, PS walls are inclined such that the angle the wall makes with the underlying surface is not 90°. The difference between the ideal case of rectangular channel (Figure 7a) and the real system (Figure 7b) is depicted in Figure 7, where R is the radius of curvature. If we let θ_i be the angle of inclination as shown in Figure 7b, then eq 7 should be modified to

$$h_c = L\left|\frac{1-\sin(90+\theta-\theta_i)}{\cos(90+\theta-\theta_i)}\right| \tag{8}$$

To determine the experimental values of θ_i, the PB phase was removed selectively using *n*-hexane, which dissolves PB but not PS. Cross-sectional AFM profiles of the remaining PS phase were then obtained as shown

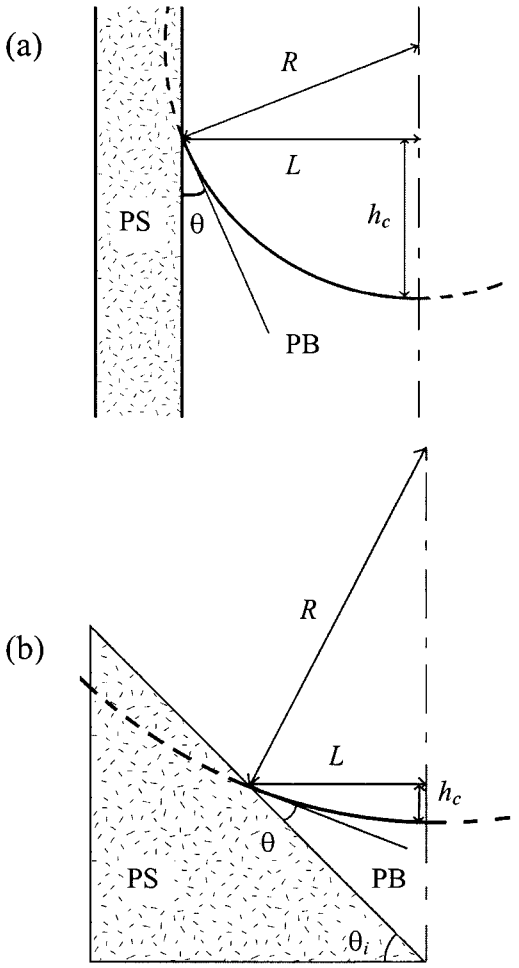

Figure 7. (a) Schematic diagram for meniscus formation of PB in the idealized rectangular PS channel. (b) Schematic diagram for meniscus formation of PB in the real PS channel.

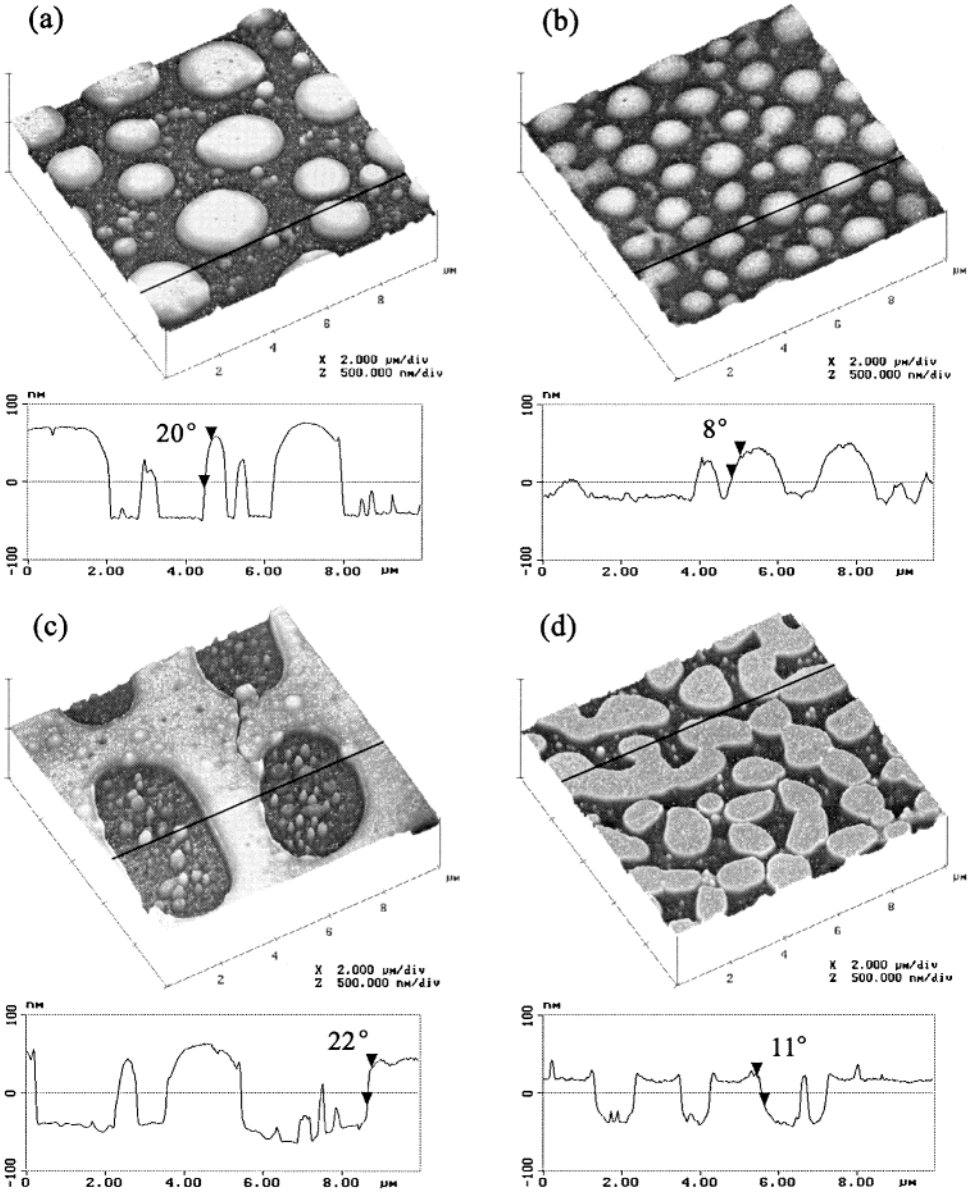

Figure 8. (a) Magnified three-dimensional and cross-sectional AFM images of PS/PB (50/50) blend film 120 nm thick. (b) Magnified three-dimensional and cross-sectional AFM images of PS/PB (50/50) blend film 60 nm thick. (c) Magnified three-dimensional and cross-sectional AFM images of PS/PB (65/35) blend film 120 nm thick. (d) Magnified three-dimensional and cross-sectional AFM images of PS/PB (65/35) blend film 60 nm thick.

in Figure 8. The angles were determined using the two arrows shown in each of the cross-sectional profiles. It is notable that the angle depends on the film thickness. For the thicker film (120 nm), the angle ranged from 18° to 23° whether the blend is symmetric (Figure 8a) or asymmetric (Figure 8c), whereas for the thinner film (60 nm), it ranged from 6° to 12° (Figure 8b for the symmetric and Figure 8d for the asymmetric blend). A higher inclination angle for a thicker film can also be observed elsewhere[4] where the system was the PS/PMMA blend.

Another factor to consider is the half channel width L. The length that is equivalent to L in the case of symmetric blend is half the distance between two adjacent PS domains, and it is half the domain (dark domains in Figure 8c,d) size in the case of the asymmetric blend. An average value can be used in eq 8. For the thin film (60 nm), an average of 500 nm was obtained. When this value is used in eq 8 along with the corresponding inclination angle, a capillary rise of 40−67 nm results for the thin film. Similarly for the thick film, a capillary rise of 35−52 nm can be calculated from eq 8 with 2 μm for the average value of L.

Because of nonidealities involved, the calculated values are just estimates. Nevertheless, it is quite interesting that the ranges of the estimates for both thin and thick films are similar, and they are in the range of the experimental value of approximately 50 nm. The ranges are similar due to the compensating dependence of the inclination angle and the equivalent length L on the film thickness. A thicker film leads not only to a larger L but also to a larger inclination angle, which compensate for each other in eq 8.

In summary, we have found that there is a capillary rise of mobile PB into the void of an elastomeric mold, as expected, when 60 nm thick films of PS/PB blends are annealed with the mold in place. On the other hand, the mobile PB under the void of the mold recedes instead of rising with almost no PB left when 120 nm thick films of the blends are annealed under the

identical annealing conditions as for the 60 nm thick films. This contrasting behavior has been shown to depend on whether a complete wetting of immobile PS phase by the mobile PB takes place: formation of protruding strips when complete wetting takes place and that of recessed strips when a partial wetting occurs such that PB cannot make contact with the walls of the void of the elastomeric mold. Since the height that PB can rise to by wetting of PS is fixed for fully developed meniscus, the degree of wetting, complete or partial, is determined by the trough to hill distance of PS phase. An examination of the surface structure of the as-cast films shows that there is a height difference between PS and PB phases with PS protruding. This distance turns out to be 30−40 nm for the 60 nm thick films whereas it is 60−70 nm for 120 nm thick films, which indicates that the distance between the highest and lowest points of the fully developed meniscus is about 50 nm. To get an estimate of the capillary rise, the equation for the capillary rise was modified to account for the angle PS walls make with the underlying surface. The equation yields an estimate in the range of the experimental value of approximately 50 nm.

When the thickness of a film is less than 100 nm, long-range force of van der Waals interactions dominates. With the wetting taking place, however, the long-range force cannot compete with the short-range force of wetting. Therefore, in the initial stage of the structure formation, wetting dominates. Once a fully developed meniscus forms, the question for the system under consideration is whether the PB meniscus formed by wetting of PS makes contact with the over-capping void walls of the mold in place. If the contact is made, the short-range force of capillarity takes over once again, and mobile PB forms a new meniscus on the walls of the void. When the contact is not made, only the long-range force acts on PB under the void of the mold. This long-range force, which causes dewetting, is responsible for the formation of recessed patterns.

References and Notes

(1) Bruder, F.; Brenn, R. *Phys. Rev. Lett.* **1992**, *69*, 624−627.
(2) Tanaka, H. *Phys. Rev. Lett.* **1993**, *70*, 2770−2773.
(3) Dalnoki-Veress, K.; Forrest, J. A.; Stevens, J. R.; Dutcher, J. R. *J. Polym. Sci., Part B* **1996**, *34*, 3017−3024.
(4) Tanaka, K.; Takahara, A.; Kajiyama, T. *Macromolecules* **1996**, *29*, 3232−3239.
(5) Walheim, S.; Boltau, M.; Mlynek, J.; Krausch, G.; Steiner, U. *Macromolecules* **1997**, *30*, 4995−5003.
(6) Dalnoki-Veress, K.; Forrest, J. A.; Dutcher, J. R. *Phys. Rev. E* **1998**, *57*, 5811−5817.
(7) Newby, B. Z.; Composto, R. J. *Macromolecules* **2000**, *33*, 3274−3282.
(8) Martin, P.; Brochard-Wyart, F. *Phys. Rev. Lett.* **1998**, *80*, 3296−3299.
(9) Brochard-Wyart, F.; Martin, P.; Redon, C. *Langmuir* **1993**, *9*, 3682−3690.
(10) Sharma, A. *Langmuir* **1993**, *9*, 861−869.
(11) Suh, K. Y.; Kim, Y. S.; Lee, H. H. *Adv. Mater.* **2001**, *13*, 1386−1389.
(12) Orts, W. J.; Zanten, J. H.; Wu, W.; Satija, S. K. *Phys. Rev. Lett.* **1993**, *71*, 867−870.
(13) Forrest, J. A.; Dalnoki-Veress, K.; Dutcher, J. R. *Phys. Rev. E* **1997**, *56*, 5705−5716.
(14) Reiter, G. *Phys. Rev. Lett.* **1992**, *68*, 75−78.
(15) David, M. O.; Reiter, G.; Sitthai, T.; Schultz, J. *Langmuir* **1998**, *14*, 5667−5672.
(16) Ivanov, I. B. *Thin Liquid Films: Fundamentals and Applications*; Marcel Dekker: New York, 1998.
(17) Israelachivili, J. N. *Intermolecular and Surface Forces*; Academic Press: London, 1992.
(18) de Gennes, P. G. *Rev. Mod. Phys.* **1985**, *57*, 827−863.
(19) Curry, J. E.; Christenson, H. K. *Langmuir* **1996**, *12*, 5729−5735.
(20) Barnes, K. A.; Karim, A.; Douglas, J. F.; Nakatani, A. I.; Gruell, H.; Amis, E. J. *Macromolecules* **2000**, *33*, 4177−4185.
(21) Adamson, A. W.; Gast, A. P. *Physical Chemistry of Surfaces*; Wiley-Interscience: New York, 1997.

MA011602L